RESEARCH

Suppression of tomato wilt by cell-free supernatants of *Acinetobacter baumannii* isolates from wild cacao from the Colombian Amazon

Carolina Pisco-Ortiz[1] · Adriana González-Almario[2] · Liz Uribe-Gutiérrez[3] · Mauricio Soto-Suárez[3] ·
Carol V. Amaya-Gómez[1]

Abstract

Tomato vascular wilt caused by *Fusarium oxysporum* f. sp. *lycopersici* (*Fol*) is one of the most limiting diseases of this crop. The use of fungicides and varieties resistant to the pathogen has not provided adequate control of the disease. In this study, siderophore-producing bacteria isolated from wild cocoa trees from the Colombian Amazon were characterized to identify prominent strategies for plant protection. The isolates were taxonomically classified into five different genera. Eight of the fourteen were identified as bacteria of the *Acinetobacter baumannii* complex. Isolates *CBIO*024, *CBIO*086, *CBIO*117, *CBIO*123, and *CBIO*159 belonging to this complex showed the highest efficiency in siderophore synthesis, producing these molecules in a range of 91–129 μmol/L deferoxamine mesylate equivalents. A reduction in disease severity of up to 45% was obtained when plants were pretreated with *CBIO*117 siderophore-rich cell-free supernatant (SodSid). Regarding the mechanism of action that caused antagonistic activity against *Fol*, it was found that plants infected only with *Fol* and plants pretreated with SodSid *CBIO*117 and infected with *Fol* showed higher levels of *PR1* and *ERF1* gene expression than control plants. In contrast, *MYC2* gene expression was not induced by the SodSid *CBIO*117 application. However, it was upregulated in plants infected with *Fol* and plants pretreated with SodSid *CBIO*117 and infected with the pathogen. In addition to the disease suppression exerted by SodSid *CBIO*117, the results suggest that the mechanism underlying this effect is related to an induction of systemic defense through the salicylic acid, ethylene, and priming defense via the jasmonic acid pathway.

✉ Carol V. Amaya-Gómez
  camaya@agrosavia.co

1 Centro de Investigación La Libertad, Corporación
   Colombiana de Investigación Agropecuaria – Agrosavia,
   Villavicencio, Meta, Colombia

2 Facultad de Ciencias Agrarias, Universidad Nacional de
   Colombia, Bogotá, Colombia

3 Centro de investigación Tibaitatá, Corporación Colombiana
   de Investigación Agropecuaria-Agrosavia, Mosquera,
   Cundinamarca, Colombia

Graphical abstract
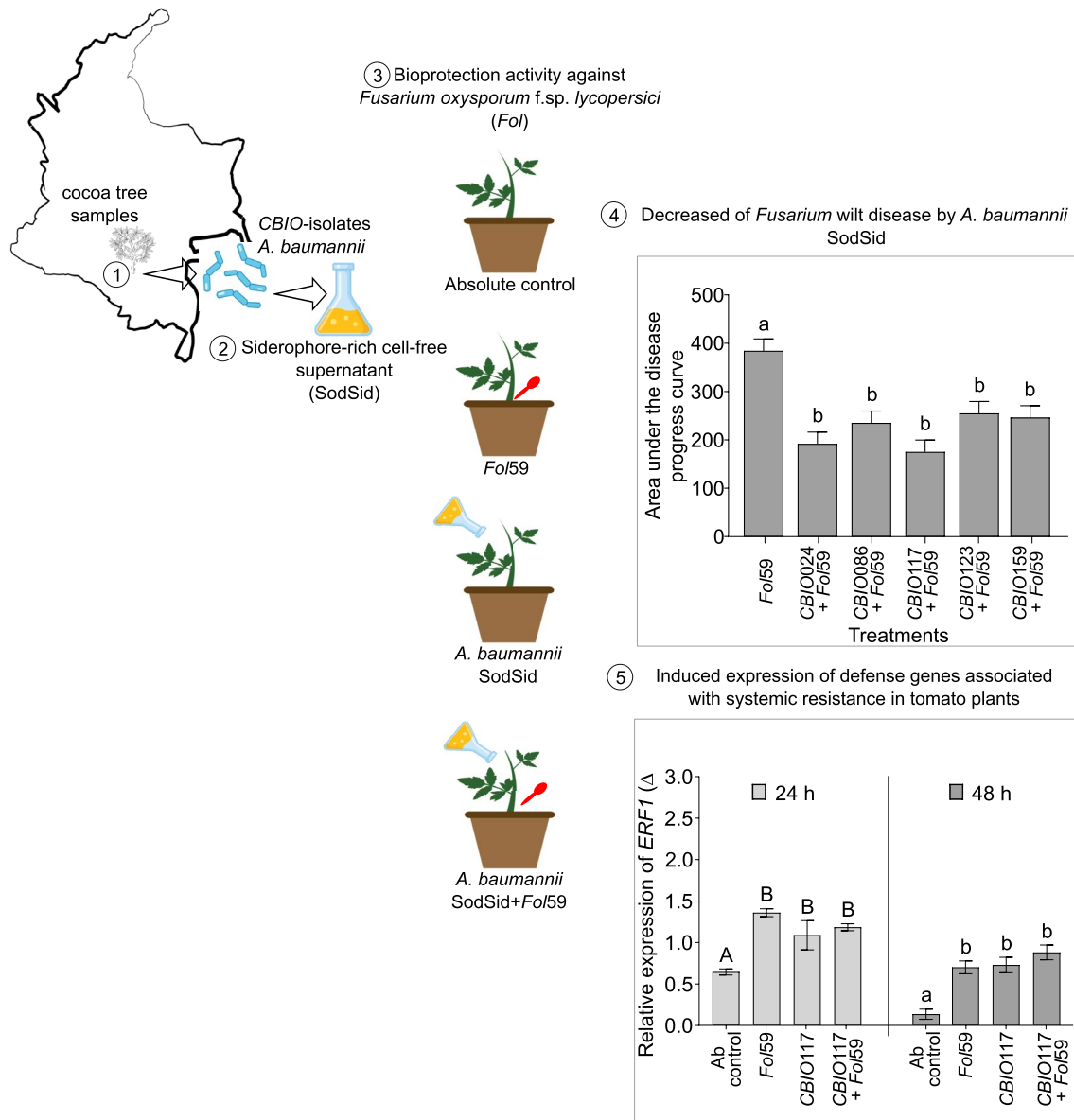
Introduction

Tomato vascular wilt, caused by *Fusarium oxysporum* f. sp. *lycopersici* (*Fol*), is one of the most destructive diseases, causing qualitative and quantitative losses (Atif et al. 2021). Currently, several management strategies are available to control *Fol*, including the use of fungicides and plant-resistant varieties (Amini and Dzhalilov 2010). However, chemical treatment is only available as a protective barrier for seeds (Bodah 2017), and the treatment with agrochemicals to control *Fol* is avoided due to their persistence in soil and their toxicity to beneficial organisms (Yu et al. 2017). Consequently, recent research on its management has focused on alternative strategies such as disease-suppressive soils, beneficial microorganisms, and induction of host resistance (McGovern 2015; Mwangi et al. 2019).

The interest in bacteria for biological control has increased during the last years. These microorganisms

exhibit biocontrol of plant diseases, inhibiting the growth of a wide range of plant pathogenic fungi, through the production of siderophores, antimicrobial compounds, and lytic enzymes, and by inducing plant defense responses (Moreno et al. 2018; Karthika et al. 2020). Following exposure to pathogens or beneficial microorganisms, plants activate defense responses both locally and systemically (Mauch-Mani et al. 2017). These responses are associated with Systemic Acquired Resistance (SAR) and Induced Systemic Resistance (ISR). ISR by beneficial microbes is commonly based on priming (Mauch-Mani et al. 2017). Priming is defined as a state of enhanced protection characterized by faster and stronger defense responses against environmental stresses (Martínez-Medina et al. 2016). During beneficial plant–microbe interaction, priming is expressed at the transcriptional level, for instance, elevated levels of expression of *AP2/ERF* family transcription factors have been observed. Several members of this family belong to the signaling cascade that is part of the Jasmonic Acid (JA) and Ethylene (ET)-mediated defense responses (Van der Ent et al. 2009).

Siderophores are iron-chelating agents produced by bacteria, fungi, and plants (Soares 2022). These molecules play a role in the solubilization of iron from minerals that are found as part of insoluble complexes. The excretion of these molecules allows bacteria to sequester the available iron and transport it into the cell. In the environment, the ferric form of iron is insoluble and physiologically unavailable. Microorganisms have evolved to synthesize siderophores that have a high affinity for ferric iron. These ferric iron-siderophore complexes are transported to the cytosol and then reduced to ferrous iron to be accessible to microorganisms (Saha et al. 2016). Siderophore production in *Acinetobacter* and other bacteria genera is regulated by the concentration of available iron in the growth medium. Maindad et al. (2014) showed that the synthesis of an acinetobactin-like siderophore produced by *Acinetobacter calcoaceticus* strain HIRFA32 decreases as iron concentration increases. Similarly, the catechol activity of *Acinetobacter baumannii* siderophores was found to reach 70% at a concentration of 20 μM of $FeCl_3$ and decreased to 45% at 80 μM of $FeCl_3$ (Modarresi et al. 2015). In *Bacillus anthracis,* while production of the siderophore bacillibactin was found to be highly regulated by the concentration of available iron, petrobactin synthesis is likely regulated by additional virulence-related factors (Lee et al. 2011). Dumas et al. (2013) described that *Pseudomonas aeruginosa* switches from the pyochelin production under highly iron-limiting conditions, pyoverdine production when a moderate iron concentration is available.

Besides siderophore's role as iron-bearers, these molecules have been reported to have an antifungal effect or to induce the activation of the plant defense responses, including the activation of ISR (Dellagi et al. 2009; Santoyo et al. 2010; Aznar and Dellagi 2015). Several studies have shown that different siderophore-producing *Pseudomonas* species, under low iron conditions, are associated with plant protection against pathogens, including, *Botrytis cinerea*, *Colletotrichum lindemuthianum*, *Pythium splendens*, *Pseudomonas syringae*, *Magnaporthe oryzae* and *Fusarium oxysporum* (Buysens et al. 1996; Meziane et al. 2005; De Boer et al. 2007; De Vleesschauwer et al. 2008; Aznar et al. 2014). In addition, results obtained by Yu et al. (2011) showed that treatment with bacillibactin, a catechol-like siderophore produced by *Bacillus subtilis* CAS15, resulted in a 50% disease reduction in pepper during infection with *Fusarium oxysporum* f. sp. *capsica*. These studies demonstrated that siderophores can (i) trigger ISR-mediated resistance and/or (ii) suppress the pathogen by uptake of iron from the environment. Recent reports indicate that siderophore-triggered ISR involves the accumulation of reactive oxygen species and phenolic compounds, and the activation of hormone signaling pathways particularly those mediated by ET and JA.

In view of the few studies that have conducted to explore the biological diversity and attributes of microorganisms adapted to megadiverse areas such as the Amazon rainforest (Guerra et al. 2020), this study aimed to characterize siderophore-producing bacteria isolated from this region and to identify promising candidates for the suppression of tomato vascular wilt caused by *Fol*. The expression level of gene markers from the JA, ET, and salicylic acid signaling pathways was measured to better understand the mechanism of antagonistic action exerted by siderophore-rich cell-free supernatant applied to plants.

Materials and methods

Bacteria isolates and physiological characterization

The fourteen bacterial isolates used in this study (*CBIO*021, *CBIO*024, *CBIO*086, *CBIO*101, *CBIO*117, *CBIO*118, *CBIO*120, *CBIO*121, *CBIO*123, *CBIO*127, *CBIO*133, *CBIO*142, *CBIO*149, and *CBIO*159) were previously isolated from rhizosphere and phyllosphere samples collected from wild cocoa trees (*Theobroma subincanum* Mart.*, Theobroma cacao* L. and *Herrania nitida* (Poepp.) R.E. Shult.) from the Colombian Amazon. The isolates were deposited in the microbial germplasm bank of Agrosavia. The sampling coordinates are shown in Table S1. Isolates were characterized by Gram staining (Gram 1884). Lactose fermentation was visualized on MacConkey agar (Oxoid, MacConkey, 1985) where individual colonies were plated and incubated at 37 °C for 48 h in the dark. Hemolytic activity was determined qualitatively using blood agar culture medium (Oxoid) containing 5% v/v bovine blood (Lányi, 1987). After 24 h of incubation at 37 °C, the presence around the

inoculum site of green or translucent halos, or the absence of halo was interpreted as alpha-hemolysis, beta-hemolysis or gamma-hemolysis, respectively. Experiments were performed in triplicate.

Quantification of siderophore production

Siderophore production was evaluated in iron-free modified minimal medium (MM) (Robertsen et al. 1981) containing: $C_5H_8NNaO_4$, 2.42 g/L; $C_6H_{12}O_6$, 10 g/L; supplemented with stock solution 10 mL/L of K_2HPO_4, 3 mg/mL; KH_2PO_4, mg/mL; $CaCl_2 \cdot 6H_2O$, 0.5 mg/mL; NaCl, 0.5 mg/mL; $MgSO_4$, 1,5 mg/mL; pH 7.0). The cell mass of a 24-h culture of each isolate was used to inoculate MM broth to an initial optical density (OD) of 0.2 at 600 nm. The cell culture was incubated at 28 °C under constant shaking at 117 rpm for 72 h with an oscillation diameter of 25 mm (Tecnal®, incubator shaker TE-421, Brazil). The cell-free supernatant was collected by centrifugation at 8273×g for 15 min at 4 °C (Eppendorf®, centrifuge 5430, Germany). Detection of siderophores was estimated by Chrome Azurol Sulfonate (CAS) colorimetric test, as described by Schwyn and Neilands, (1987). Briefly, 500 µL of the culture supernatant were mixed with 500 µL of CAS solution (As). After incubation for 1 h in the dark at room temperature, the OD was measured at 630 nm. MM broth without inoculum mixed with CAS solution was used as a control (Ar). Siderophore production was expressed as a color change of the reaction from blue to orange and was calculated by the following equation: $[(Ar - As)/Ar] * 100$. Where Ar represents the absorbance of the control and As represents the absorbance of the sample. To estimate the siderophore concentration, a standard calibration curve was performed using deferoxamine mesylate (DFOM) as an iron chelator following the methodology described by Radzki et al. (2013) and Mehnert et al. (2017). The concentration was expressed in µmol/L DFOM equivalents. According to Radzki et al. (2013) 1 mmol of DFOM captures 56 mg of Fe^{3+}.

Taxonomic identification and phylogeny

The total deoxyribonucleic acid (DNA) from the fourteen selected isolates was extracted from grown cultures using the MoBio PowerLyzer® UltraClean® Microbial Kit (Carslbad, CA) following the manufacturer's instructions. The 16S V4 of the ribosomal ribonucleic acid (rRNA) gene was amplified by polymerase chain reaction (PCR). The PCR reaction mixture consisted of 5 µL of DNA template, 1 µL (10 µM) of the primers 515F (5′-GTGYCAGCMGCCGCGGTAA-3′) and 806R (5′-GGACTACNVGGGTWTCTAAT-3′) (Apprill et al. 2015; Parada et al. 2016), 10 µL of Go Taq® Green Master Mix (Promega) and 8 µL of nuclease-free water (Invitrogen™). Amplification was carried out by an initial

denaturation step at 94 °C for 3 min, followed by 35 cycles of 45 s of denaturation at 94 °C, 60 s of annealing at 50 °C and 90 s of extension at 72 °C (Applied Biosystems SimpliAmp, Thermal Cycler, USA). Final extension was carried out at 72 °C for 10 min. The resulting amplification products were separated using a 1% w/v agarose gel. Sequencing of the amplified DNA fragments was performed by Corpogen Corporation (https://www.corpogen.org/, Bogotá. Colombia). To resolve ambiguous bases on the forward and reverse trace files, the resulting sequences were manually checked considering the PHRED scores received. Taxonomic identification of isolates to genus level was carried out using the NCBI GenBank database (https://blast.ncbi.nlm.nih.gov) and the basic local alignment search analysis tool (BLASTn). The resultant unrooted tree topology was evaluated by bootstrap analyses (Felsenstein 1985) of the neighbor-joining method based on 1000 bootstrap replicates. Trees were rooted using the partial sequence of the 16S rRNA gene of *Lactococcus plantarum* (NR_044358.1) as an outgroup.

Identification of *Acinetobacter* species by Vitek 2 system compact

The eight isolates identified as *Acinetobacter* sp. were cultured in Luria–Bertani media (LB) for 24 h at 35 °C. A sterile swab was used to transfer and suspend the cell mass in 3.0 mL of sterile saline solution (0.45% NaCl, pH 7.0) in a test tube. The turbidity of the cell suspension was measured and adjusted to the McFarland turbidity range between 0.50 and 0.63 using a DensiChekTM Plus (VITEK® 2, BioMereux, USA). The identification GN ID cards (Ref 21341, VITEK® 2 GN) were inoculated with each microorganism's cell suspension using a Vitek 2 Compact® (BioMerieux, Lyon, France). All cards were incubated at 35 °C for 18 h. Each test reaction was read every 15 min to measure turbidity and colored products of substrate metabolism. Interpretation of the results was carried out as described by Pincus (2006) where the GN card is based on established biochemical methods for the identification of isolates gram-negative bacilli.

Induction of siderophores production

The production of siderophores in five *A. baumannii* isolates that showed increased ability to excrete these molecules (*CBIO*024, *CBIO*086, *CBIO*117, *CBIO*123, and *CBIO*159) was evaluated in MM broth without iron, and in MM containing a low (22 µM) and a high (220 µM) concentration of $FeCl_3 \cdot 6H_2O$. A bacterial inoculum was prepared by culturing the selected bacteria on nutrient agar for 24 h at 28 °C. The cell mass was then washed twice with NaCl (0.85% w/v) by centrifugation for 5 min at 4430×g (Hermle, centrifuge Z 326 k, Germany), removing the supernatant between washes.

The resulting cell pellet was resuspended in MM broth supplemented with each of the FeCl$_3$·6H$_2$O concentrations and adjusted to a final OD of 2.0 at 600 nm (Thermo Fisher Scientific, Genesys 150 spectrophotometer, USA). Next, a 0.5 mL aliquot of each bacterial inoculum was added to Falcon tubes (15 mL) containing 4.5 mL of the MM broth without iron or supplemented with FeCl$_3$·6H$_2$O, until a final OD of 0.2 at 600 nm was reached. Cell cultures were incubated at 28 °C under constant shaking at 180 rpm with an oscillation diameter of 10 mm for 72 h (Heidolph, Shakers Unimax 1010, Germany). Siderophore production was quantified using CAS assay as described above. Three biological replicates were performed in a series of 4 samples.

Bioactivity assays against *Fol*

The bioactivity of the cell-free supernatant of the five *A. baumannii* isolates *CBIO*024, *CBIO*086, *CBIO*117, *CBIO*123, and *CBIO*159 was evaluated against *Fol* by in vivo experiments on tomato plants. For this purpose, the pathogen *Fusarium oxysporum* f. sp. *lycopersici* Race 2 identified as *Fol*59 was used in this study (Carmona et al. 2020; Yu et al. 2022).

Cell-free supernatant of each isolate with high content of siderophores (SodSid) was produced in MM without iron using the methodology described above. For this experiment, twenty-eight days old seedlings of the susceptible tomato cultivar Santa Cruz Kada grown in a growth chamber at a temperature of 28 °C, with a relative humidity of 60% and a photoperiod of 14 h of light and 10 h of darkness were used. Plants were treated by drenching with 10 mL of SodSid of each isolate. Forty-eight hours after SodSid treatment, plants were removed from the seedbed and infected with *Fol*59 by root immersion into a suspension of 1×10^5 microconidia/mL (Carmona et al. 2020). Subsequently, the plants were transplanted into 16 oz pots containing soil and sand in a 2:1 ratio. Treatments consisted of plants inoculated only with SodSid of *A. baumannii* isolates (*CBIO*024, *CBIO*086, *CBIO*117, *CBIO*123, and *CBIO*159) and plants inoculated with SodSid and infected with *Fol*59 (*CBIO*024 + *Fol*59, *CBIO*086 + *Fol*59, *CBIO*117 + *Fol*59, *CBIO*123 + *Fol*59, and *CBIO*159 + *Fol*59). Water-treated plants were considered as absolute control (Ab control), and plants infected with *Fol*59 (*Fol*59) were used as pathogen control. The experimental setup was a randomized complete factorial design with two factors. The first factor corresponded to the five bacterial supernatants, the second to plants with or without the pathogen infection, for a total of 10 treatments and two controls. Three biological replicates were performed. Each biological replicate comprised three technical replicates, and each technical replicate consisted of eleven plants. Selected parameters related to pathogenicity, plant growth, and regulation of ISR-associated genes were evaluated.

Disease incidence and severity were recorded periodically for 21 days. To assess disease severity, the scale proposed by Rongai et al. (2017) was used and modified as follows: absence of symptoms was recorded as level 0; slight yellowing appearance of one or two leaves was recorded as level 1; necrotic lesions formed both, at the base of the stem and on internodes in the center of the plant, with or without the yellowing appearance of basal and median leaves were recorded as level 2; total yellowing appearance of basal leaves, with some wilted leaves and necrotic lesions in the steam extending upwards was recorded as level 3; loss of turgor and wilting of the plant was recorded as level 4; a dead plant was recorded as level 5. The severity index (SI) and area under the disease progression curve (AUDPC) were calculated using the equations described by Chiang et al. (2017) and Pedroza-Sandoval and Gaxiola (2009). The plant height, dry weight, and chlorophyll content of plants were determined 16 days post-inoculation with *Fol*59 (dpi). The plant height was recorded using a tape measure. The weight of six plants per treatment was measured after drying in an oven at 60 °C for 72 h. Chlorophyll content was estimated in Soil Plant Analysis Development (SPAD) units using the Minolta® SPAD 502 chlorophyll meter. Leaf chlorophyll content was measured in the distal part of the adaxial side of an apical leaf (three measurements) (Hurtado et al. 2017), values shown are means ± SE (n = 11) plants, using the mean of three measurements per plant.

Quantification of the transcription of systemic resistance-related genes

The relative expression of three defense marker genes was calculated by quantitative Real-Time Reverse Transcription Polymerase Chain Reaction (qRT-PCR). The treatments evaluated were (i) non-inoculated plants treated with water (Ab control), (ii) plants only inoculated with *CBIO*117 SodSid (*CBIO*117), (iii) plants only infected with *Fol*59 (*Fol*59, pathogen control), and iv) plants inoculated with *CBIO*117 SodSid and infected with *Fol*59 (*CBIO*117 + *Fol*59). The differential expression of *PR1*, *ERF1*, and *MYC2* genes associated with SA, ET, and Jasmonic acid (JA), respectively, was assessed at 24 and 48 h post infection with *Fol* (hpi). For this, specific primers previously reported for *PR1, ERF1,* and *MYC2* were used, additionally, elongation factor expression (EF1a) was used as a reference (Table 1) (Martínez-Medina et al. 2013).

Total RNA extraction was performed following the protocol described by Yockteng et al. (2013). Complementary DNA (cDNA) synthesis was performed using the ProtoScript® II First Strand cDNA kit (New England BioLabs) following the manufacturer's recommended protocol. Quantitative RT-PCR reactions were performed using the IqTM SYBR® Green Supermix kit (Bio-Rad®)

Table 1 Primer sequences for defense marker genes in qPCR analysis

Primer	Sequence (5′–3′)	References
LePR1aqF	GTGGGATCGGATTGATATCCT	Martínez-Medina et al. (2013)
LePR1aqR	CCTAAGCCACGATACCATGAA	
LeERF1qF	GAGGGGTCCTTGGTCTCTACTC	Huang et al. (2004)
LeERF1qR	ACAGCAGCTGGAGATAATCCAT	
LeMYC2qF	AGCAGGAGCATCGGAAGAA	Martínez-Medina et al. (2013)
LeMYC2qR	CCAAATCGGGCTGGAACTA	
LeEF1aqF	GATTGGTGGTATTGGAACTGTC	Martínez-Medina et al. (2013)
LeEF1aqR	AGCTTCGTGGTGCATCTC	

in a final volume of 10 μL per reaction. The reaction mixture consisted of 2 μL of cDNA, 0.4 μL of each primer (0.4 μM), 5 μL of 2X of IQ SYBR Green Supermix, and 2.2 μL of molecular grade water. Reactions were performed in duplicate for each of the three independent biological replicates. To analyze the relative gene expression data, the common-base method proposed by Ganger et al. (2017) was used according to the following equation: $\Delta Ct = ((Log)_{10}E_{ref} \times Ct_{ref}) - ((Log)_{10}E_{Goi} \times Ct_{Goi})$ where E_{ref} is the efficiency of the housekeeping gene $EF1a$, E_{Goi} is the efficiency of the target gene, and Ct are threshold values of the cycle.

Antimicrobial activity test in dual-liquid culture assay

To test antimicrobial activity by the dual-liquid culture method, 50 mL of iron-deficient media containing glucose at 5% w/v (IDM, Muller et al. 1984) was taken in a 250-mL culture flask and inoculated with 50 mL of *CBIO*117 inoculum (10^7 cells/mL) and a 5 mm size PDA plug of freshly grown *Fol*59. The culture flasks were incubated at 28 °C for 72 h on a rotary shaker at 120 rpm with an oscillation diameter of 19 mm (Max^Q 4000, Barnstead/Lab-line, Switzerland). *Fol*59 cultures without *CBIO*117 inoculum were used as controls. After incubation, cell culture supernatants were filtered through a Whatman No. 1 filter paper (1001-055, Whatman) and dried at 60 °C. *Fol*59 biomass growth on both cultures, co-inoculated with *CBIO*117 and control (without *CBIO*117), was compared to assess the antagonistic activity of *CBIO*117. The percentage reduction in fungal biomass was calculated by the equation: $Inhibition(\%) = \frac{(W_1 - W_2)}{w_1 \times 100}$ where W_1 corresponds to the biomass (g) of *Fol*59 in the control culture, while W_2 corresponds to the biomass of *Fol*59 grown in co-culture with *CBIO*117 (Basha and Ulaganathan 2002; Trivedi et al. 2008).

Statistical analysis

To evaluate the effect of treatments on disease severity, a linear mixed-effects model analysis was performed. Treatment, sampling day, biological replication, and interaction were considered fixed effects. The experimental unit (plant) was included as a random effect (Schandry 2017). Relative chlorophyll content was analyzed using linear mixed-effects models. Plant height and dry weight values were analyzed by ANOVA and Tukey test. Tukey tests for pairwise comparisons of means were performed at a significance level of $P < 0.05$. Relative expression levels were analyzed using cycle threshold values calculated by univariate analysis at each post-inoculation time point (Popović et al. 2021). All statistical analyses were carried out using R software (version 4.1.2).

Results

Phenotypic characterization of bacterial isolates

The fourteen isolates used in this study were previously selected for their ability to produce siderophores. For each isolate, geographic location, plant part for sample collection (rhizosphere or phyllosphere), and phenotypic characteristics are shown in Table 2. The isolates showed differential microscopic characteristics and ability to ferment lactose and lyse blood cells. Two isolates were Gram-positive bacilli, eight were Gram-negative coccobacilli, and four were Gram-negative bacilli. The lactose utilization assay showed that most isolates fermented lactose as observed by the appearance of a clear halo around colonies. The greatest diversity was found in the hemolytic activity test, in which isolates showing α, β, and γ activity were identified.

Quantification of siderophore production

Comparison of siderophore production among 14 siderophore-producing isolates showed significant differences ($P < 0.05$, Fig. 1). The concentration of siderophores ranged from 2.7 μM ± 0.3 (*CBIO*101) to 129.9 μM ± 19.1 (*CBIO*123). Isolates *CBIO*024, *CBIO*086, *CBIO*123, *CBIO*117, and *CBIO*159 showed the highest siderophore production. For these isolates, siderophore concentrations were 99 ± 6.2, 91 ± 7.6, 129 ± 19.1, 107 ± 5.8, and

Table 2 Geographical location, plant part of sample collection (rhizosphere or phyllosphere) and phenotypic characteristics of isolates analyzed in this study

Isolate code	Isolation origin			Phenotypic characteristics			
	Location	Plant part	Plant Host	Gram stain	Morphology	Lactose	Hemolysis
CBIO021	Caquetá	Rh	*T. subincanum*	G+	Bacilli	Ng	β
CBIO024	Caquetá	Rh	*T. subincanum*	G−	Cocco	−	γ
CBIO086	Caquetá	Phl	*T. subincanum*	G−	Cocco	+	γ
CBIO101	Caquetá	Rh	*T. subincanum*	G−	Bacilli	−	α
CBIO117	Putumayo	Rh	*T. subincanum*	G−	Cocco	−	γ
CBIO118	Caquetá	Rh	*T. subincanum*	G−	Bacilli	−	γ
CBIO120	Putumayo	Phl	*T subincanum*	G−	Bacilli	−	γ
CBIO121	Putumayo	Phl	*H. nitida*	G+	Bacilli	Ng	β
CBIO123	Putumayo	Rh	*T. subincanum*	G−	Cocco	+	γ
CBIO127	Putumayo	Phl	*T. subincanum*	G−	Cocco	+	γ
CBIO133	Putumayo	Phl	*T. cacao*	G−	Cocco	+	α
CBIO142	Putumayo	Phl	*T. cacao*	G−	Bacilli	+	γ
CBIO149	Putumayo	Phl	*T. cacao*	G−	Cocco	+	β
CBIO159	Caquetá	Phl	*T. cacao*	G−	Cocco	+	γ

Rh rhizosphere, *Phl* phyllosphere, *Coccobacilli* Cocco, *G+* Gram positive, *G-* Gram negative, *Ng* absence of growth
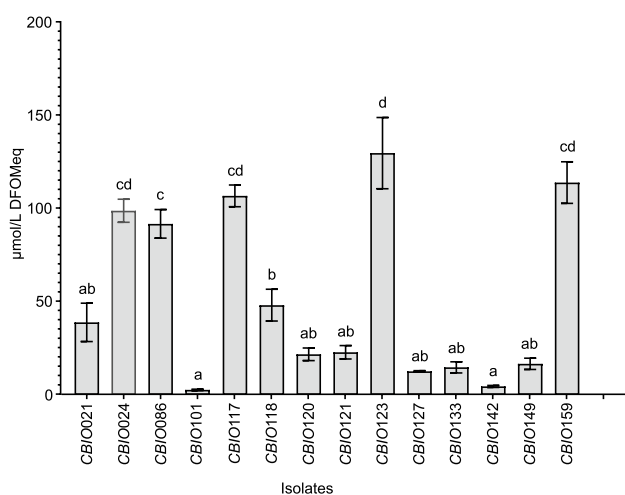

Fig. 1 Production of siderophores by *CBIO*-isolates (expressed in μmol/L equivalents of DFOM) after 72 h after incubation. Bacteria were grown in minimal media without iron. Values followed by the same letter do not differ significantly (Tukey test, $P < 0.05$). Values correspond to the mean ($\pm$ES) of three biological replicates with n = 3

isolates to genus level. These analyses classified the isolates into 14 genera, eight belonging to the *Acinetobacter* genus, two to the *Bacillus* genus, one to the *Delftia* genus, one to the genus *Herbaspirillum*, one to the genus *Pseudomonas*, and one to the genus *Serratia* (Fig. 2).

Vitek tests were performed to further characterize the taxonomic identity of the *CBIO* isolates classified within the genus *Acinetobacter*. Isolates *CBIO*024, *CBIO*086, *CBIO*117, *CBIO*123, *CBIO*159, *CBIO*120, *CBIO*127, and *CBIO*149 were classified within the *A. baumannii* complex with a 99% of probability. All these isolates showed five different metabolic patterns (Group 1, 2, 3, 4, and 5; Fig. 3). Most of them were able to grow using D-cellobiose, D-glucose, D-mannose, tyrosine arylamidase, L-lactate, succinate, and coumarate as carbon source. *CBIO*117 was the only isolate unable to grow using citrate as the sole carbon source, and inorganic ammonium salt as the sole source of nitrogen. Remarkably, *CBIO*117, *CBIO*123, and *CBIO*159 did not assimilate L-histidine and were the isolates with the highest siderophore production. In contrast, isolates *CBIO*120, *CBIO*127, and *CBIO*149 showed lower production of iron chelators and did not grow in the presence of urease (Fig. 3).

A. baumannii isolates *CBIO*024, *CBIO*086, *CBIO*117, *CBIO*123, and *CBIO*159 were selected for further studies, based on their increased ability to produce siderophores and differences in metabolic profile compared to other isolates.

114 ± 11.1 μmol/L DFOM equivalents, respectively (Fig. 1). For isolates identified as *Delftia* and *Pseudomonas* (*CBIO*101 and *CBIO*142), low concentrations of siderophore (4.6 ± 0.5 μmol/L DFOM equivalents) were observed (Fig. 1 and Fig. 2).

Taxonomic characterization

Comparison of the partial 16S rRNA gene sequence and phylogeny analysis allowed taxonomic identification of the

Effects of cell-free supernatants of *A. baumanii* isolates on the suppression of vascular wilt

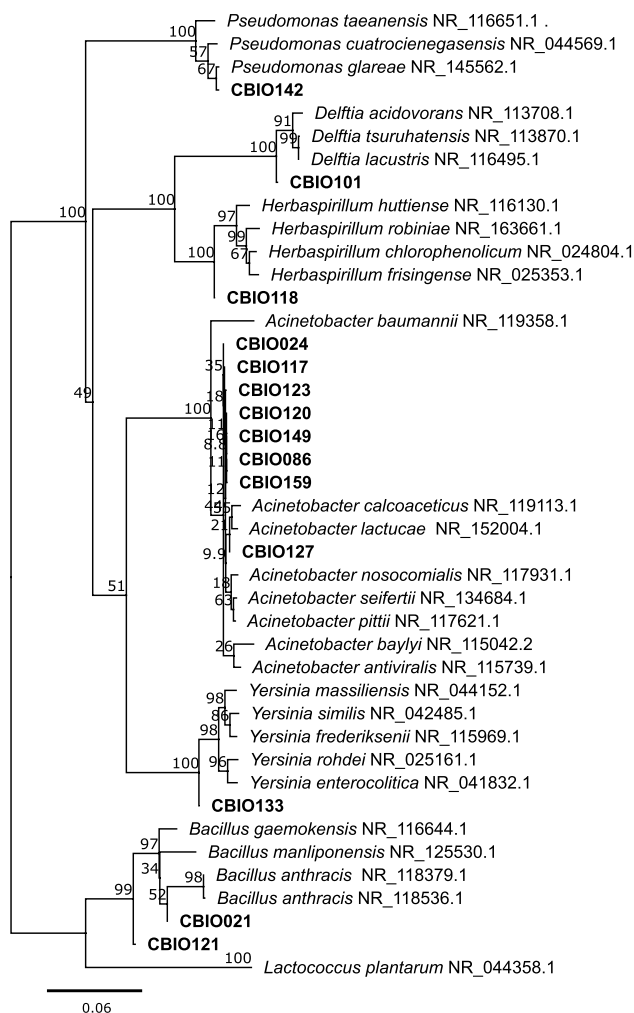We further confirmed the effect cell-free supernatants of *A. baumanii* on plant protection against *Fol*. To ensure

Fig. 2 Phylogenetic-tree construction using the neighbor-joining method. The phylogenetic analysis was performed with partial 16S rRNA gene sequences. Bootstrap values, expressed as percentages of 1000 replications, are shown at branch points. The numbers above the branches indicate the percentage of consensus support. Bold letters highlight the *CBIO*-isolates characterized in this study. The tree was rooted using *Lactococcus plantarum* NR_044358.1 as an outgroup

that bioactivity assays were performed with siderophore-rich supernatants, siderophores production was evaluated in MM containing different concentrations of $FeCl_3 \cdot 6H_2O$. The results showed that at higher iron concentrations, siderophore production decreased (Figure S1). When *A. baumannii* isolates *CBIO*024, *CBIO*086, *CBIO*117, *CBIO*123, and *CBIO*159 were culture in MM without iron, we found that the mean concentration of siderophores production was 43 μmol/L DFMO equivalents. Thus, activities against tomato *Fusarium* wilt were attempted using the cell-free supernatant of selected *CBIO*-isolates grown under iron-starved conditions (SodSid).

Preventive application of SodSid of *A. baumanii* isolates reduced disease incidence in plants infected with *Fol*59

by 31% (*CBIO*024 + *Fol*59), 11% (*CBIO*086 + *Fol*59), 33% (*CBIO*117 + *Fol*59), 24% (*CBIO*123 + *Fol*59) and 20% (*CBIO*159 + *Fol*59) relative to plants only infected with the pathogen, where 100% incidence was reached at 21 dpi. Disease severity index and AUDPC of plants pre-treated with SodSid and subsequently infected with *Fol*59 (*CBIO* + *Fol*59) were lower compared to plants infected only with *Fol*59. However, at 21 dpi, the highest disease suppression was observed in *CBIO*117 + *Fol*59 treatment wheredisease severity was reduced up to 45% (Fig. 4B).

Growth parameters of tomato plants treated with cell-free supernatant of *A. baumannii* isolates

Next, we investigated whether *A. baumannii* SodSid affected plant development rate. The plant height at 16 dpi was significantly delayed ($P < 0.05$) in *Fol*59-infected plants compared to water-only treated plants (Ab control plants), which showed greater increase in height, and higher relative chlorophyll content (Table 3). Interestingly, plants treated only *CBIO*117 SodSid showed the greatest plant height, with significant differences with respect to the other treatments ($P < 0.05$). Plants treated with SodSid of isolate *CBIO*024, SodSid of *CBIO*123 and infected with *Fol*59 (*CBIO*123 + *Fol*59), and plants infected only with *Fol*59 showed lower amounts of total dry matter accumulation. As for the SPAD chlorophyll index, significantly higher SPAD units were observed in all plants treated with SodSid from *CBIO*-isolates and plants treated with SodSid of the *CBIO*-isolates and then infected with *Fol*59, compared to Ab and *Fol*59 control plants ($P < 0.05$).

Effect of SodSid on the expression of defense marker genes in *Fol*-infected tomato plants

To determine whether the reduction of wilt disease severity in tomato plants treated with SodSid from *A. baumannii CBIO*117 is related to the induction of plant defense genes, the relative expression of the *PR1, ERF1*, and *MYC2* genes was evaluated in plants treated only with SodSid from *CBIO*117 isolate and plants pretreated with SodSid and subsequently infected with *Fol*59. Two separate time points were considered after infection with *Fol*59 (24- and 48-h post-infection (hpi)). At the earliest time (24 hpi), there was no significant difference in *PR1* expression levels between treatments. However, at 48 hpi all plants, including those treated only with SodSid from *A. baumannii CBIO*117 showed a significant up-regulation of *PR1* gene ($P < 0.05$) (Fig. 5A). These results indicate SodSid application of *A. baumannii CBIO*117 is able to induce plant defense responses, including *PR1*-based basal immunity (Fig. 5A).

Similarly, *ERF1* gene expression levels increased in both conditions, after treatment *CBIO*117 SodSid alone and in

Fig. 3 Metabolic profile using ID-GNB card of the VITEK 2 system for taxonomic identification of the *Acinetobacter* sp. isolates. Presence of growth (+), absence of growth (−). Ala-phe-pro-arylamidase (APPA), Adonitol (ADO), L-pyrrolydonyl-arylamidase (PyrA), L-arabitol (IARL), D-cellobiose (dCEL), Beta-galactosidase (BGAL), H2S production (H2S), Beta-N-acetyl-glucosaminidase (BNAG), Glutamyl arylamidase pNA (AGLTp), D-glucosa (dGLU), Gamma-glutamyl transferase (GGT), Fermentation of glucose (OFF), Beta-glucosidase (BGLU), D-maltose (dMAL), D-mannitol (dMAN), D-mannose (dMNE), Beta-xylosidase (BXYL), Beta-alanine arylamidase pNA (BAIap), L-proline-arylamidase (ProA), Lipase (LIP), Palatinose (PLE), Tyrosine arylamidase (TyrA), Urease (URE), D-sorbitol (dSOR), Saccharose/sucrose (SAC), D-tagatose (dTAG), D-trehalose (dTRE), Citrate (Sodium) (CIT), Malonate (MNT), 5-Keto-D-gluconate (5 KG), L-lactate alkalinization (ILATk), Alpha-glucosidase (AGLU), Succinate alkalinization (SUCT), Beta-N-acetyl galactosaminidase (NAGA), Alpha-galactosidase (AGAL), Phosphatase (PHOS), Glycine arylamidase (GlyA), Ornithine descarboxylase (ODC), Lysine decarboxylase (LDC), L-histidine assimilation (IHISa), Cumarate (CMT), Beta-glucuronidase (BGUR), O/129 Resistance (comp.vibrio.) (O129R), Glu-Gly-Arg-arylamidase (GGAA), L-malate assimilation (IMLTa), Ellman (ELLM), L-lactate assimilation (ILATa)

Substrate	Isolate							
	CBIO024	CBIO086	CBIO117	CBIO123	CBIO159	CBIO120	CBIO127	CBIO149
	Presence of growth							
APPA	−	−	−	−	−	−	−	−
ADO	−	−	−	−	−	−	−	−
PyrA	−	−	−	−	−	−	−	−
IARL	−	−	−	−	−	−	−	−
dCEL	+	+	+	+	+	+	+	+
BGAL	−	−	−	−	−	−	−	−
H2S	−	−	−	−	−	−	−	−
BNAG	−	−	−	−	−	−	−	−
AGLTp	−	−	−	−	−	−	−	−
dGLU	+	+	+	+	+	+	+	+
GGT	−	−	−	−	−	−	−	−
OFF	−	−	−	−	−	−	−	−
BGLU	−	−	−	−	−	−	−	−
dMAL	−	−	−	−	−	−	−	−
dMAN	−	−	−	−	−	−	−	−
dMNE	+	+	+	+	+	+	+	+
BXYL	−	−	−	−	−	−	−	−
BAlap	−	−	−	−	−	−	−	−
ProA	−	−	−	−	−	−	−	−
LIP	−	−	−	−	−	−	−	−
PLE	−	−	−	−	−	−	−	−
TyrA	+	+	+	+	+	+	+	+
URE	+	+	+	+	+	−	−	−
dSOR	−	−	−	−	−	−	−	−
SAC	−	−	−	−	−	−	−	−
dTAG	−	−	−	−	−	−	−	−
dTRE	−	−	−	−	−	−	−	−
CIT	+	+	−	+	+	+	+	+
MNT	−	−	−	−	−	+	+	+
5KG	−	−	−	−	−	−	−	−
ILATk	+	+	+	+	+	+	+	+
AGLU	−	−	−	−	−	−	−	−
SUCT	+	+	+	+	+	+	+	+
NAGA	−	−	−	−	−	−	−	−
AGAL	−	−	−	−	−	−	−	−
PHOS	−	−	−	−	−	−	−	−
GlyA	−	−	−	−	−	−	−	−
ODC	−	−	−	−	−	−	−	−
LDC	−	−	−	−	−	−	−	−
IHISa	+	+	−	−	−	+	+	+
CMT	+	+	+	+	+	+	+	+
BGUR	−	−	−	−	−	−	−	−
O129R	−	−	−	−	−	+	+	+
GGAA	−	−	−	−	−	−	−	−
IMLTa	+	−	−	−	−	−	−	−
ELLM	−	−	−	−	−	−	−	−
ILATa	+	−	−	−	−	−	−	−
Group	1	2	3	4	4	5	5	5

plants pretreated with SodSid and subsequently infected with *Fol*59, compared with control plants. This means that the preventive application on tomato roots with SodSid of *CBIO*117 promoted ethylene-mediated defense responses in tomato plants (Fig. 5B).

Expression of the *MYC2* transcription factor was not induced after preventive SodSid application of *A. baumannii CBIO*117 on tomato roots. The highest level of *MYC2* expression occurred at 24 hpi in plants infected only with *Fol*59, followed by plants pretreated with SodSid and then infected with the pathogen (*CBIO*117 + *Fol*59). However, at 48 hpi, a decrease in *MYC2* gene expression was detected in plants infected with *Fol*59, whereas the gene expression was maintained in plants previously stimulated with the SodSid and infected with the pathogen (*CBIO*117 + *Fol*59).

Antimicrobial activity assay in dual culture in liquid medium

To gain further insight into the antimicrobial activity of *A. baumannii CBIO*117, we performed an assay using the dual culture method in a liquid medium. It was observed that *CBIO*117 isolate was not able to inhibit the growth of *Fol*59. No significant differences ($P < 0.05$) were observed when comparing *Fol*59 biomass growth in either culture, co-inoculated with *CBIO*117 (0.20 ± 0.08 g/mL) or the control culture without *CBIO*117 (0.22 ± 0.06 g/mL).

Discussion

The tomato crop is threatened by wilt caused by *Fusarium oxysporum* f. sp. *Lycopersici*. Increasing attention is being paid to reducing the use of synthetic fungicides to control plant diseases, mainly because of their negative impact on production costs, environmental pollution, risks to human health, development of fungicide resistance, and post-harvest fruit quality. The use of beneficial microorganisms or their metabolites is a promising alternative for disease management. In this study, siderophore-producing bacteria

Fig. 4 Effect of preventive application of cell-free supernatant from *A. baumanii* isolates on *Fusarium* wilt of tomato. **A** Disease severity index. **B** Effect of SodSid from five *Acinetobacter* sp. isolates on AUDPC severity at 21 days post inoculation. **C** Representative images of tomato plants treated with water (Ab control), infected with *Fol*59 (*Fol*59), and plants previously treated with *CBIO*117 SodSid, subsequently infected with *Fol*59 (*CBIO*117+*Fol*59). Values correspond to the mean of three biological replicates with n = 15. Value means followed by the same letter do not differ significantly (Tukey test, P < 0.05)
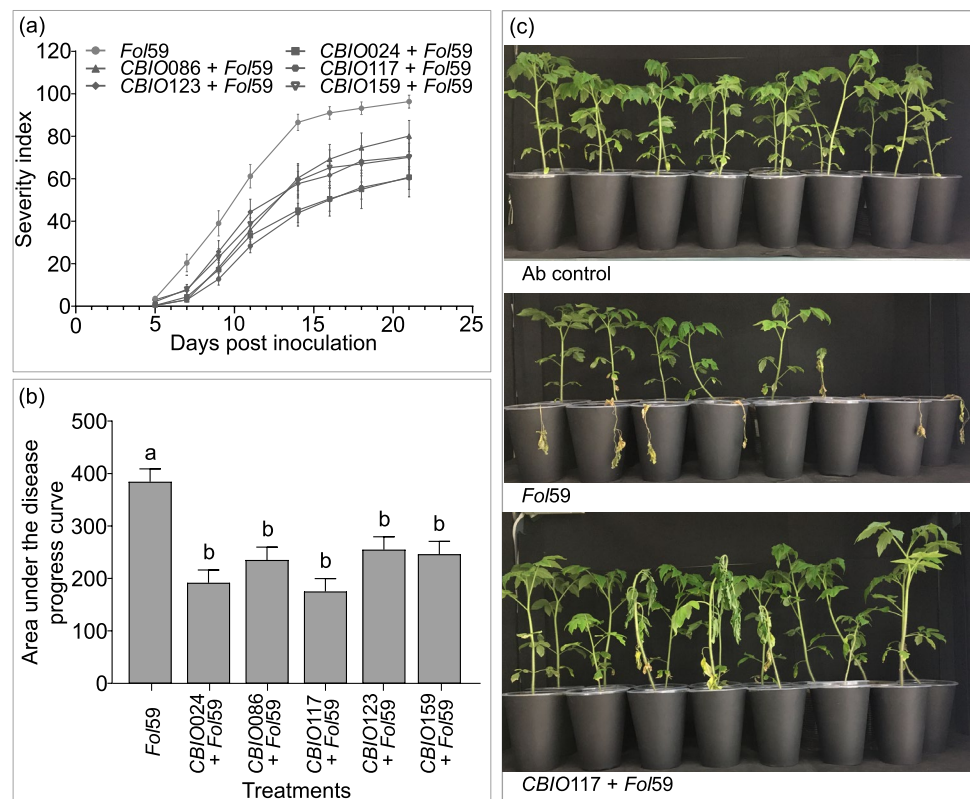
Table 3 Growth parameters of tomato plants treated with cell-free supernatant of *A. baumannii* isolates

Treatments	Plant height* (cm)	Dry weight* (mg)	Chlorophyll* (SPAD)
Ab control	20.6 ± 0.5^{Aa}	190 ± 0.02^{Aab}	24.7 ± 0.3^{Aa}
*CBIO*024	20.2 ± 0.5^{Aa}	120 ± 0.02^{Aa}	26.2 ± 0.3^{Ab}
*CBIO*086	21.8 ± 0.5^{Aab}	170 ± 0.02^{Aab}	26.2 ± 0.3^{Ab}
*CBIO*117	23.5 ± 0.5^{Ab}	220 ± 0.02^{Ab}	27.1 ± 0.3^{Ab}
*CBIO*123	21.6 ± 0.5^{Aab}	180 ± 0.02^{Aab}	27.1 ± 0.3^{Ab}
*CBIO*159	21.3 ± 0.5^{Aa}	170 ± 0.02^{Aab}	27.0 ± 0.3^{Ab}
*Fol*59	19.5 ± 1.0^{Ba}	90 ± 0.02^{Aa}	22.8 ± 0.3^{Ba}
*CBIO*024 + *Fol*59	18.8 ± 0.6^{Ba}	170 ± 0.02^{Aab}	24.3 ± 0.3^{Bb}
*CBIO*086 + *Fol*59	19.7 ± 0.7^{Ba}	130 ± 0.02^{Aab}	24.3 ± 0.3^{Bb}
*CBIO*117 + *Fol*59	19.5 ± 0.6^{Ba}	160 ± 0.02^{Aab}	25.2 ± 0.3^{Bb}
*CBIO*123 + *Fol*59	18.4 ± 0.7^{Ba}	90 ± 0.02^{Aa}	25.2 ± 0.3^{Bb}
*CBIO*159 + *Fol*59	18.3 ± 0.7^{Ba}	140 ± 0.02^{Aab}	25.1 ± 0.3^{Bb}

*Each variable was analyzed independently. Absolute control (Ab control), plants infected with *Fol*59 (*Fol* 59). The mean (+ES) of plant height and relative chlorophyll content values correspond to three biological replicates with n = 15. The mean (+ES) of dry weight values correspond to three biological replicates with n = 6. Value means followed by the same letter do not differ significantly (Tukey test, P < 0.05). Capital letters show the significant differences between plants not infected and infected with *Fol*59. Lower-case letters show significant differences between the treatments and their respective control

from the rhizosphere and phyllosphere of wild cocoa trees collected in the Colombian Amazon were characterized. Furthermore, the bioactivity of the cell-free supernatants containing siderophores was tested against *Fol*.

Fourteen isolates showed high siderophore production, of which eight were identified as *A. baumannii*. Several structurally distinct siderophores have been described for this bacterium including acinetobactin, baumannoferrins A and B and, fimsbactins A–F. A large collection of well-characterized siderophores has been also described in the same bacterial genus where the remaining *CBIO*-isolates were classified. For instance, serobactin A, B, and C from
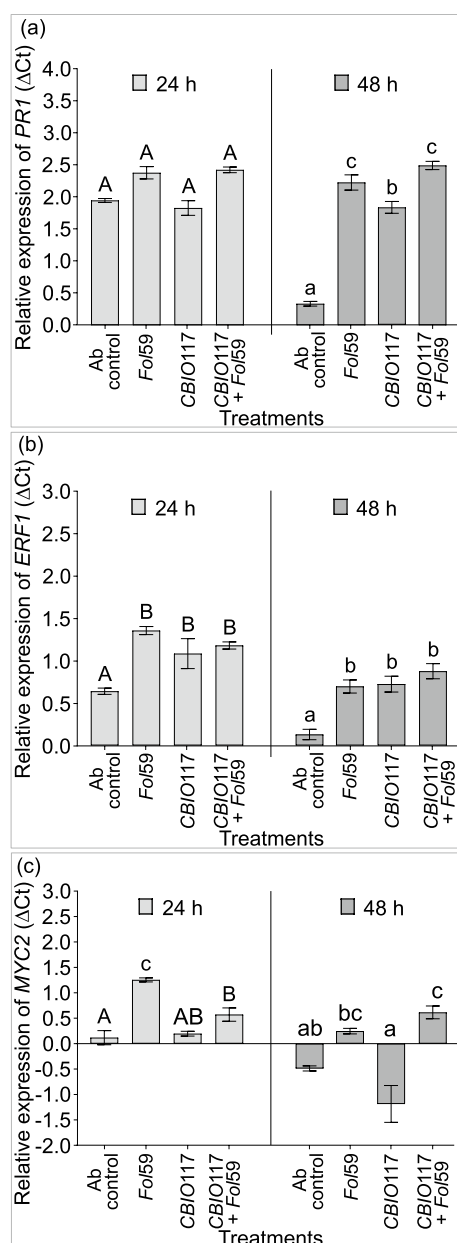
Fig. 5 Relative expression of defense genes to assess the effect of cell-free supernatant (SodSid) of *A. baumannii CBIO*117 on the activation of tomato defense responses. **A** Relative expression of *PR1* gene. **B** Relative expression of the *ERF1* gene, and **C** Relative expression of *MYC2* gene. Treatments correspond to plants treated with water (Ab control), plants infected with *Fol*59 (Fol59), plants treated with SodSid of *CBIO*117 isolate (*CBIO*117), and plants treated with SodSid of *CBIO*117 and then infected with *Fol*59 (*CBIO*117 + *Fol*59). Values correspond to the mean (±ES) of two biological replicates with n = 2. Means of values followed by the same letter do not differ significantly (Tukey test, $P < 0.05$)

Herbaspirillum (Rosconi et al. 2013; Tejman-Yarden et al. 2019), bacillibactin and petrobactin from *Bacillus* (Wilson et al. 2006), serratiochelin, chrysobactin, aerobactin, and enterobactin from *Serratia* (Ehlert et al. 1994; Weakland

et al. 2020), and pyoverdine, ferrioxamine, piocheln, and ferribactin from *Pseudomonas* (Aguilar et al. 2021). The production of several structurally diverse iron chelators by the same bacteria has been associated with improved iron acquisition and prevention of iron deprivation under different environmental conditions, facilitating the uptake of other metals, and contributing to competitiveness (McRose et al. 2018). Given that the *CBIO*-isolates were isolated in iron-depleted media, it could be considered that the ability to produce structurally diverse siderophores favors the prevalence of the *A. baumannii* isolates, explaining why a higher representative number of isolates from this genus was obtained. To better understand the ability of *CBIO*-isolates to survive under iron-limited conditions, their growth and persistence under iron deficient and iron-abundant conditions need to be evaluated.

Plant protection activity of *Acinetobacter* sp. bacteria against phytopathogenic filamentous fungi and bacteria has been reported before (Xue et al. 2009; Safdarpour and Khodakaramian 2018; Foughalia et al. 2022; Khalil et al. 2021). Different molecules are associated with suppression of these fungi, including siderophores, gibberellic— and indole acetic acids, volatile compounds, or microbial enzymes such as chitinases and proteases. In this study, the application of cell-free supernatant reduced the incidence and severity of the *Fusarium* wilt of tomato. Further studies are needed to better understand the metabolites present in the supernatant of the *CBIO*-isolates that generated the plant protection activity. However, as these supernatants were rich in siderophores, it is possible that the antagonistic activity was at least partially generated by these molecules. Prashant et al. (2009) demonstrated the antifungal activity of catechol-like siderophores from *Acinetobacter calcoaceticus* strain SCW1 against *Aspergillus flavus*, *Aspergillus niger*, *Colletotrichum capsicum*, and *F. oxysporum*. Sayyed and Reddy (2011) reported the growth inhibitory potential of siderophore-rich cell-free supernatants obtained from *Acinetobacter* sp. SH-94B isolate against *A. niger* NCIM 1025, *A. flavus* NCIM 650, *F. oxysporum* NCIM 1281, *Alternaria alternata* ARI 715, *Cercospora arachichola*, *Metarhizium anisopliae* NCIM 1311 and *Ralstonia solanacerum* NCIM 5103. Bacterial siderophores have already shown to play a role in antagonizing plant pathogens through iron deprivation, but also by activating plant-induced systemic resistance (Höfte and Bakker 2007; Betoudji et al. 2020). A synthetic siderophore of fimsbactin-like structure produced by *Acinetobacter* sp. was reported as an iron-bearer under iron deprivation conditions and induce systemic priming in *Arabidopsis thaliana* (Betoudji et al. 2020). Since siderophore-rich cell-free supernatants from *CBIO*-isolates were used, the hypothesis regarding competition for iron as a plant protection mechanism seems unlikely. However, as the cell supernatant was applied before infection with *Fol*59, and

gene expression analysis showed differences between plants inoculated with the supernatants alone (SodSid) with respect to absolute control plants, the bioactivity could be better explained by induction of systemic resistance. In addition, the absence of antimicrobial activity was observed when *CBIO*117 supernatant was directly confronted against *Fol*, indicating that disease suppression might not be associated with the action of antimicrobial compounds.

Plants respond to biotic stresses caused by pathogens and pests through a localized defense response at the site of infection or, sometimes, by a systemic response known as SAR. However, some beneficial microorganisms that mainly inhabit the rhizosphere can induce systemic resistance in the plant to counteract phytopathogen attack and strengthen physiological processes (Romera et al. 2019). Secretion of molecules such as siderophores by beneficial microorganisms has been shown to improve plant nutrition and trigger plant defense response (Verbon et al. 2017). In this study, SodSid *CBIO*117 activated SA and ET signaling pathways in tomato plants, as evidenced by changes in gene expression of *PR1* and *ERF1*. These genes did not decrease in expression after infection with the pathogen. However, early expression of *PR1* and *ERF1* in plants only infected with the pathogen could be associated with PAMP-triggered immunity, in which PR1 protein accumulation could potentially restrain the pathogen and induce activation of defense-related pathways (Boccardo et al. 2019). These results suggest that the application of siderophore-rich cell-free supernatants prior to pathogen infection elicits a transient systemic response to counteract plant pathogen attack via the AS and ET signaling pathways. Interestingly, no changes were detected in the expression of the *MYC2* gene marker of the jasmonic acid pathway upon SodSid *CBIO*117 application. However, when plants previously treated with SodSid were infected with *Fol*59, the *MYC2* gene increased expression levels. This response may be associated with an induction of priming defense, reinforcing plant defenses against pathogen attack.

In conclusion, this study demonstrates that siderophore-rich cell-free supernatants of *A. baumannii CBIO*117 can activate systemic resistance in tomato plants and could generate a priming-type defense against *Fol*. This siderophore-producing bacterium could be, in the near future, a potential biocontrol agent to control plant diseases. To elucidate the hormonal signaling pathway involved in the plant protection response, evaluation of additional genes involved in systemic resistance is recommended.

Declarations

Conflict of interest The authors declare that they have no conflict of interest.

References

Aguilar MO, Álvarez F, Medeot D, Jofré E, Semorile L, Pistorio M (2021) Screening of epiphytic rhizosphere-associated bacteria in Argentinian Malbec and Cabernet-Sauvignon vineyards for potential use as biological fertilisers and pathogen-control agents. OENO One 55(4):145–157. https://doi.org/10.20870/oeno-one.2021.55.4.4655

Amini J, Dzhalilov FS (2010) The effects of fungicides on *Fusarium oxysporum* f. sp. *lycopersici* associated with fusarium wilt of tomato. J Plant Prot Res 50(2):172–178. https://doi.org/10.2478/v10045-010-0029-x

Apprill A, McNally S, Parsons R, Weber L (2015) Minor revision to V4 region SSU rRNA 806R gene primer greatly increases detection of SAR11 bacterioplankton. Aquat Microb Ecol. https://doi.org/10.3354/ame01753

Atif M, Riaz R, Batool A, Yasmin H, Nosheen A, Naz R, Nadeem M (2021) Glucanolytic rhizobacteria associated with wheat-maize cropping system suppress the Fusarium wilt of tomato (*Lycopersicum esculentum* L.). Sci Hortic 287:110275. https://doi.org/10.1016/j.scienta.2021.110275

Aznar A, Dellagi A (2015) New insights into the role of siderophores as triggers of plant immunity: what can we learn from animals? J Exp Bot 66(11):3001–3010. https://doi.org/10.1093/jxb/erv155

Aznar A, Chen N, Rigault M, Riache N, Joseph D, Desmaële D, Mouille G, Boutet S, Soubigou-Taconnat L, Renou J-P, Thomine S, Expert D, Dellagi A (2014) Scavenging iron: a novel mechanism of plant immunity activation by microbial siderophores.

Plant Physiol 164(4):2167–2183. https://doi.org/10.1104/pp.113.233585

Basha S, Ulaganathan K (2002) Antagonism of *Bacillus* species (strain BC121) towards *Curvularia lunata*. Curr Sci 82(12):1457–1463

Betoudji F, Abd El Rahman T, Miller MJ, Ghosh M, Jacques M, Bouarab K, Malouin F (2020) A Siderophore Analog of Fimsbactin from *Acinetobacter* hinders growth of the phytopathogen *Pseudomonas syringae* and induces systemic priming of immunity in *Arabidopsis thaliana*. Pathogens 9(10):806. https://doi.org/10.3390/pathogens9100806

Boccardo NA, Segretin ME, Hernandez I, Mirkin FG, Chacón O, Lopez Y, Borrás-Hidalgo O, Bravo-Almonacid FF (2019) Expression of pathogenesis-related proteins in transplastomic tobacco plants confers resistance to filamentous pathogens under field trials. Sci Rep 9:2791. https://doi.org/10.1038/s41598-021-95177-2

Bodah ET (2017) Root rot diseases in plants: a review of common causal agents and management strategies. Agri Res Tech. https://doi.org/10.19080/artoaj.2017.05.555661

Buysens S, Heungens K, Poppe J, Hofte M (1996) Involvement of pyochelin and pyoverdin in suppression of *Pythium*-induced damping-off of tomato by *Pseudomonas aeruginosa* 7NSK2. Appl Environ Microbiol 62(3):865–871. https://doi.org/10.1093/jxb/erv155

Carmona SL, Burbano-David D, Gómez MR, Lopez W, Ceballos N, Castaño-Zapata J, Simbaqueba J, Soto-Suárez M (2020) Characterization of pathogenic and nonpathogenic *Fusarium oxysporum* isolates associated with Commercial tomato crops in the andean region of Colombia. Pathogens 9(1):70. https://doi.org/10.3390/pathogens9010070

Chiang KS, Liu HI, Tsai JW, Tsai JR, Bock CH (2017) A discussion on disease severity index values. Part II: using the disease severity index for null hypothesis testing. Ann Appl Biol 171:490–505. https://doi.org/10.1111/aab.12396

De Boer M, Bom P, Kindt F, Keurentjes JJ, Van Der Sluis I, Van Loon L, Bakker P (2007) Control of Fusarium wilt of radish by combining *Pseudomonas putida* strains that have different disease-suppressive mechanisms. Phytopathology 93(5):626–632. https://doi.org/10.1094/PHYTO.2003.93.5.626

De Vleesschauwer D, Djavaheri M, Bakker P, Höfte M (2008) *Pseudomonas fluorescens* WCS374r-induced systemic resistance in rice against *Magnaporthe oryzae* is based on pseudobactin-mediated priming for a salicylic acid-repressible multifaceted defense response. Plant Physiol 148(4):1996–2012. https://doi.org/10.1104/pp.108.127878

Dellagi A, Segond D, Rigault M, Fagard M, Simon C, Saindrenan P, Expert D (2009) Microbial siderophores exert a subtle role in Arabidopsis during infection by manipulating the immune response and the iron status. Plant Physiol 150(4):1687–1696. https://doi.org/10.1104/pp.109.138636

Dumas Z, Ross-Gillespie A, Kümmerli R (2013) Switching between apparently redundant iron-uptake mechanisms benefits bacteria in changeable environments. Proc Biol Sci 280(1764):20131055. https://doi.org/10.1098/rspb.2013.1055

Ehlert G, Taraz K, Budzikiewicz H (1994) Serratiochelin, a new catecholate siderophore from *Serratia marcescens*. Zeitschrift Für Naturforschung C 49(1–2):11–17. https://doi.org/10.1515/znc-1994-1-203

Felsenstein J (1985) Phylogenies and the comparative method. Am Nat 125(1):1–15

Foughalia A, Yousra B, Chandeysson C, Djedidi M, Tahirine M, Kamel A, Nicot P (2022) *Acinetobacter calcoaceticus* SJ19 and *Bacillus safensis* SJ4, two Algerian rhizobacteria protecting tomato plants against *Botrytis cinerea* and promoting their growth. Egypt J Biol Pest Control. https://doi.org/10.1186/s41938-022-00511-z

Ganger MT, Dietz GD, Ewing SJ (2017) A common base method for analysis of qPCR data and the application of simple blocking in qPCR experiments. BMC Bioinform 18(1):534. https://doi.org/10.1186/s12859-017-1949-5

Gram H (1884) Uber die isolierte Färbung der Schizomyceten in Schnitt-und Trockenpräparaten. Fortschr Med 2:185–189

Guerra CA, Heintz-Buschart A, Sikorski J, Chatzinotas A, Guerrero-Ramírez N, Cesarz S, Beaumelle L, Rillig MC, Maestre FT, Delgado-Baquerizo M, Buscot F, Overmann J, Patoine G, Phillips HRP, Winter M, Wubet T, Küsel K, Bardgett RD, Cameron EK, Eisenhauer N (2020) Blind spots in global soil biodiversity and ecosystem function research. Nat Commun 11(1):1. https://doi.org/10.1038/s41467-020-17688-2

Höfte M, Bakker P (2007) Competition for iron and induced systemic resistance by siderophores of plant growth promoting rhizobacteria. In: Microbial siderophores, pp 121–133. https://doi.org/10.1007/978-3-540-71160-5_6

Huang Z, Zhang Z, Zhang X, Zhang H, Huang D, Huang R (2004) Tomato TERF1 modulates ethylene response and enhances osmotic stress tolerance by activating expression of downstream genes. FEBS Lett 573(1–3):110–116. https://doi.org/10.1016/j.febslet.2004.07.064

Hurtado E, González-Vallejos F, Roper C, Bastías E, Mazuela P (2017) Propuesta para la determinación del contenido de clorofila en hojas de tomate. Idesia (arica) 35:129–130. https://doi.org/10.4067/S0718-34292017000400129

Karthika S, Varghese S, Jisha MS (2020) Exploring the efficacy of antagonistic rhizobacteria as native biocontrol agents against tomato plant diseases. 3 Biotech 10(7):320. https://doi.org/10.1007/s13205-020-02306-1

Khalil MdMR, Fierro-Coronado RA, Peñuelas-Rubio O, Villa-Lerma AG, Plascencia-Jatomea R, Félix-Gastélum R, Maldonado-Mendoza IE (2021) Rhizospheric bacteria as potential biocontrol agents against Fusarium wilt and crown and root rot diseases in tomato. Saudi J Biol Sci 28(12):7460–7471. https://doi.org/10.1016/j.sjbs.2021.08.043

Lányí B (1987) Classical and rapid identification methods for medically important bacteria. In: Colwell RR, Grigorova R (eds) Methods in microbiology. Current Methods for classification and identification of microorganisms, vol 19. Academic Press

Lee JY, Passalacqua KD, Hanna PC, Sherman DH (2011) Regulation of petrobactin and bacillibactin biosynthesis in *Bacillus anthracis* under iron and oxygen variation. PLoS ONE 6(6):e20777. https://doi.org/10.1371/journal.pone.0020777

Maindad DV, Kasture VM, Chaudhari H, Dhavale DD, Chopade BA, Sachdev DP (2014) Characterization and fungal inhibition activity of siderophore from wheat rhizosphere associated acinetobacter calcoaceticus strain HIRFA32. Indian J Microbiol 54(3):315–322. https://doi.org/10.1007/s12088-014-0446-z

Martínez-Medina A, Fernández I, Sánchez-Guzmán MJ, Jung SC, Pascual JA, Pozo MJ (2013) Deciphering the hormonal signalling network behind the systemic resistance induced by *Trichoderma harzianum* in tomato. Front Plant Sci 4:206. https://doi.org/10.3389/fpls.2013.00206

Martinez-Medina A, Flors V, Heil M, Mauch-Mani B, Pieterse CMJ, Pozo MJ, Ton J, Dam NM, Conrath U (2016) Recognizing plant defense priming. Trends Plant Sci 21(10):818–822. https://doi.org/10.1016/j.tplants.2016.07.009

Mauch-Mani B, Baccelli I, Luna E, Flors V (2017) Defense priming: an adaptive part of induced resistance. Annu Rev Plant Biol 68:485–512. https://doi.org/10.1146/annurev-arplant-042916-041132

McGovern RJ (2015) Management of tomato diseases caused by *Fusarium oxysporum*. Crop Prot 73:78–92. https://doi.org/10.1016/j.cropro.2015.02.021

McRose D, Baars O, Seyedsayamdost M, Morel F (2018) Quorum sensing and iron regulate a two-for-one siderophore gene cluster in *Vibrio harveyi*. Proc Natl Acad Sci 115(29):201805791. https://doi.org/10.1073/pnas.1805791115

Mehnert M, Retamal-Morales G, Schwabe R, Vater S, Heine T, Levicán G, Schlömann M, Tischler D (2017) Revisiting the chrome azurol S assay for various metal ions. Solid State Phenom 262:509–512. https://doi.org/10.4028/www.scientific.net/SSP.262.509

Meziane H, Van Der Sluis I, Van Loon L, Höfte M, Bakker P (2005) Determinants of *Pseudomonas putida* WCS358 involved in inducing systemic resistance in plants. Mol Plant Pathol 6(2):177–185. https://doi.org/10.1111/j.1364-3703.2005.00276.x

Modarresi F, Azizi O, Shakibaie MR, Motamedifar M, Mosadegh E, Mansouri S (2015) Iron limitation enhances acyl homoserine lactone (AHL) production and biofilm formation in clinical isolates of *Acinetobacter baumannii*. Virulence 6(2):152–161. https://doi.org/10.1080/21505594.2014.1003001

Moreno A, Carda V, Reyes JL, Vásquez J, Cano P (2018) Rizobacterias promotoras del crecimiento vegetal: una alternativa de biofertilización para la agricultura sustentable. Rev Colomb Biotecnol 20(1):68–83. https://doi.org/10.15446/rev.colomb.biote.v20n1.73707

Müller G, Matzanke BF, Raymond KN (1984) Iron transport in *Streptomyces pilosus* mediated by ferrichrome siderophores, rhodotorulic acid, and enantio-rhodotorulic acid. J Bacteriol 160(1):313–318. https://doi.org/10.1128/jb.160.1.313-318.1984

Mwangi MW, Muiru WM, Narla RD, Kimenju JW, Kariuki GM (2019) Management of *Fusarium oxysporum* f. sp. *lycopersici* and root-knot nematode disease complex in tomato by use of antagonistic fungi, plant resistance and neem. Biocontrol Sci. Technol. 29(3):229–238. https://doi.org/10.1080/09583157.2018.1545219

Parada AE, Needham DM, Fuhrman JA (2016) Every base matters: assessing small subunit rRNA primers for marine microbiomes with mock communities, time series and global field samples. Environ Microbiol 18(5):1403–1414. https://doi.org/10.1111/1462-2920.13023

Pedroza-Sandoval A, Gaxiola J (2009). Análisis del área bajo la curva del progreso de las enfermedades (ABCPE) en patosistemas agrícolas. In: Tópicos selectos de estadística aplicados a la fitosanidad, 1st ed., pp 180–189. https://doi.org/10.13140/2.1.4475.7767

Pincus DH (2006) Microbial identification using the bioMérieux Vitek® 2 system. Encyclopedia of rapid microbiological methods. Parenteral Drug Association, Bethesda, pp 1–32

Popović ŽD, Maier V, Avramov M, Uzelac I, Gošić-Dondo S, Blagojević D, Koštál V (2021) Acclimations to cold and warm conditions differently affect the energy metabolism of diapausing larvae of the european corn borer *Ostrinia nubilalis* (Hbn.). Front Physiol 12:768593. https://doi.org/10.3389/fphys.2021.768593

Prashant S, Makarand R, Bhushan C, Sudhir C (2009) Siderophoregenic *Acinetobacter calcoaceticus* isolated from wheat rhizosphere with strong PGPR activity. Malays J Microbiol 5(1):6–12. https://doi.org/10.21161/mjm.13508

Radzki W, Gutierrez Mañero FJ, Algar E, Lucas García JA, García-Villaraco A, Ramos Solano B (2013) Bacterial siderophores efficiently provide iron to iron-starved tomato plants in hydroponics culture. Antonie Van Leeuwenhoek 104(3):321–330. https://doi.org/10.1007/s10482-013-9954-9

Robertsen BK, Aman P, Darvill AG, McNeil M, Albersheim P (1981) The structure of acidic extracellular polysaccharides secreted by *Rhizobium leguminosarum* and *Rizobium trifolii*. Plant Physiol 67:389–400

Romera FJ, García MJ, Lucena C, Martínez-Medina A, Aparicio MA, Ramos J, Alcántara E, Angulo M, Pérez-Vicente R (2019) Induced systemic resistance (ISR) and Fe deficiency responses in dicot plants. Front Plant Sci 10:287. https://doi.org/10.3389/fpls.2019.00287

Rongai D, Pulcini P, Pesce B, Milano F (2017) Antifungal activity of pomegranate peel extract against fusarium wilt of tomato. Eur J Plant Pathol 147(1):229–238. https://doi.org/10.1007/s10658-016-0994-7

Rosconi F, Davyt D, Martínez V, Martínez M, Abin-Carriquiry JA, Zane H, Butler A, De Souza EM, Fabiano E (2013) Identification and structural characterization of serobactins, a suite of lipopeptide siderophores produced by the grass endophyte *Herbaspirillum seropedicae*. Environ Microbiol 15(3):916–927. https://doi.org/10.1111/1462-2920.12075

Safdarpour F, Khodakaramian G (2018) Assessment of antagonistic and plant growth promoting activities of tomato endophytic bacteria in challenging with *Verticillium dahliae* under in-vitro and in-vivo conditions. Biol J Microorg 7:77–90

Saha M, Sarkar S, Sarkar B, Sharma BK, Bhattacharjee S, Tribedi P (2016) Microbial siderophores and their potential applications: a review. Environ Sci Pollut Res 23(5):3984–3999. https://doi.org/10.1007/s11356-015-4294-0

Santoyo G, Valencia-Cantero E, MaDC O-M, Peña-Cabriales JJ, Farías-Rodríguez R (2010) Papel de los sideróforos en la actividad antagónica de *Pseudomonas fluorescens* ZUM80 hacia hongos fitopatógenos. Terra Latinoamericana 28:53–60

Sayyed RZ, Reddy MS (2011). Siderophore based heavy metal resistant green fungicides for sustainable environment. In: 2nd Asian PGPR proceeding, pp 443–445

Schandry N (2017) A Practical guide to visualization and statistical analysis of *R. solanacearum* infection data using R. Front Plant Sci 8:623. https://doi.org/10.3389/fpls.2017.00623

Schwyn B, Neilands JB (1987) Universal chemical assay for the detection and determination of siderophores. Anal Biochem 160(1):47–56. https://doi.org/10.1016/0003-2697(87)90612-9

Soares EV (2022) Perspective on the biotechnological production of bacterial siderophores and their use. Appl Microbiol Biotechnol 106(11):3985–4004. https://doi.org/10.1007/s00253-022-11995-y

Tejman-Yarden N, Robinson A, Davidov Y, Shulman A, Varvak A, Reyes F, Rahav G, Nissan I (2019) Delftibactin-A, a non-ribosomal peptide with broad antimicrobial activity. Front Microbiol 10:2377. https://doi.org/10.3389/fmicb.2019.02377

Trivedi P, Pandey A, Palni LMS (2008) In vitro evaluation of antagonistic properties of *Pseudomonas corrugata*. Microbiol Res 163(3):329–336. https://doi.org/10.1016/j.micres.2006.06.007

Van der Ent S, Van Hulten M, Pozo MJ, Czechowski T, Udvardi MK, Pieterse CMJ, Ton J (2009) Priming of plant innate immunity by rhizobacteria and beta-aminobutyric acid: differences and similarities in regulation. New Phytol 183(2):419–431. https://doi.org/10.1111/j.1469-8137.2009.02851.x

Verbon EH, Trapet PL, Stringlis IA, Kruijs S, Bakker P, Pieterse C (2017) Iron and immunity. Annu Rev Phytopathol 55:355–375. https://doi.org/10.1146/annurev-phyto-080516-035537

Weakland DR, Smith SN, Bell B, Tripathi A, Mobley HLT (2020) The *Serratia marcescens* siderophore serratiochelin is necessary for full virulence during bloodstream infection. Infect Immun 88(8):e00117-e120. https://doi.org/10.1128/IAI.00117-20

Wilson MK, Abergel RJ, Raymond KN, Arceneaux JEL, Byers BR (2006) Siderophores of *Bacillus anthracis*, *Bacillus cereus*, and *Bacillus thuringiensis*. Biochem Biophys Res Commun 348(1):320–325. https://doi.org/10.1016/j.bbrc.2006.07.055

Xue Q-Y, Chen Y, Li S-M, Chen L-F, Ding GC, Guo DW, Guo JH (2009) Evaluation of the strains of *Acinetobacter* and *Enterobacter* as potential biocontrol agents against *Ralstonia* wilt of tomato. Biol Control 48(3):252–258. https://doi.org/10.1016/j.biocontrol.2008.11.004

Yockteng R, Almeida AMR, Yee S, Andre T, Hill C, Specht CD (2013) A method for extracting high-quality RNA from diverse plants for next-generation sequencing and gene expression analyses. Appl. Plant Sci. 1(12):1300070. https://doi.org/10.3732/apps.1300070

Yu X, Ai C, Xin L, Zhou G (2011) The siderophore-producing bacterium, *Bacillus subtilis* CAS15, has a biocontrol effect on Fusarium wilt and promotes the growth of pepper. Eur J Soil Biol 47(2):138–145. https://doi.org/10.1016/j.ejsobi.2010.11.001

Yu S, Teng C, Liang J, Song T, Dong L, Bai X, Jin Y, Qu J (2017) Characterization of siderophore produced by *Pseudomonas syringae* BAF.1 and its inhibitory effects on spore germination and mycelium morphology of *Fusarium oxysporum*. J Microbiol 55(11):877–884. https://doi.org/10.1007/s12275-017-7191-z

Yu PL, Fulton JC, Carmona SL, Burbano-David D, Barrero LS, Huguet-Tapia JC, Soto-Suarez M (2022) Draft genome sequence and de novo assembly of a *Fusarium oxysporum* f. sp. *lycopersici* isolate collected from the Andean Region in Colombia. Microbiol. Resour. Announc. 11(1):e0098021. https://doi.org/10.1128/mra.00980-21

Publisher's Note Springer Nature remains neutral with regard to jurisdictional claims in published maps and institutional affiliations.